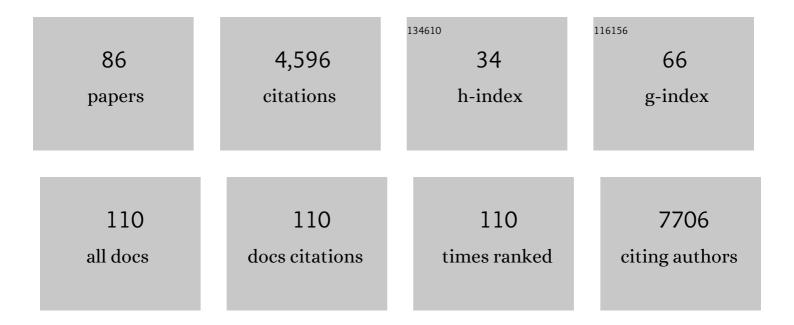
List of Publications by Year in descending order

Source: https://exaly.com/author-pdf/3290815/publications.pdf Version: 2024-02-01



#	Article	IF	CITATIONS
1	Laser ablation-single particle-inductively coupled plasma mass spectrometry as a sensitive tool for bioimaging of silver nanoparticles in vivo degradation. Chinese Chemical Letters, 2022, 33, 3484-3487.	4.8	10
2	Professor Zhifang Chai: Scientific Contributions and Achievements. Chinese Chemical Letters, 2022, , .	4.8	0
3	Multiscale Synchrotron-Based Imaging Analysis for the Transfer of PEGylated Gold Nanoparticles In Vivo. ACS Biomaterials Science and Engineering, 2021, 7, 1462-1474.	2.6	5
4	Interaction of Humic Acid with Graphene Oxide: Relation to Antibacterial Activities Against Escherichia coli. Journal of Nanoscience and Nanotechnology, 2021, 21, 1430-1438.	0.9	0
5	Iron oxide nanoparticles aggravate hepatic steatosis and liver injury in nonalcoholic fatty liver disease through BMP-SMAD-mediated hepatic iron overload. Nanotoxicology, 2021, 15, 761-778.	1.6	16
6	Polyvinylpyrrolidone functionalization induces deformable structure of graphene oxide nanosheets for lung-targeting delivery. Nano Today, 2021, 38, 101151.	6.2	16
7	Gold Nanoparticles Modified With Polyethyleneimine Disturbed the Activity of Drug-Metabolic Enzymes and Induced Inflammation-Mediated Liver Injury in Mice. Frontiers in Pharmacology, 2021, 12, 706791.	1.6	4
8	Single-Cell Isotope Dilution Analysis with LA–ICP–MS: A New Approach for Quantification of Nanoparticles in Single Cells. Analytical Chemistry, 2020, 92, 14339-14345.	3.2	30
9	Hepatic impacts of gold nanoparticles with different surface coatings as revealed by assessing the hepatic drug-metabolizing enzyme and lipid homeostasis in mice. NanoImpact, 2020, 20, 100259.	2.4	12
10	Rapamycin-Loaded mPEG-PLGA Nanoparticles Ameliorate Hepatic Steatosis and Liver Injury in Non-alcoholic Fatty Liver Disease. Frontiers in Chemistry, 2020, 8, 407.	1.8	31
11	Surface chemistry governs the sub-organ transfer, clearance and toxicity of functional gold nanoparticles in the liver and kidney. Journal of Nanobiotechnology, 2020, 18, 45.	4.2	59
12	In vivo pharmacokinetics, transfer and clearance study of graphene oxide by La/Ce dual elemental labelling method. NanoImpact, 2020, 17, 100213.	2.4	15
13	Adsorption and oxidation of SO ₂ on the surface of TiO ₂ nanoparticles: the role of terminal hydroxyl and oxygen vacancy–Ti ³⁺ states. Physical Chemistry Chemical Physics, 2020, 22, 9943-9953.	1.3	21
14	Immunological Responses Induced by Blood Protein Coronas on Two-Dimensional MoS ₂ Nanosheets. ACS Nano, 2020, 14, 5529-5542.	7.3	82
15	Elemental analysis and imaging of sunscreen fingermarks by X-ray fluorescence. Analytical and Bioanalytical Chemistry, 2019, 411, 4151-4157.	1.9	7
16	Determination of silver nanoparticles in single cells by microwell trapping and laser ablation ICP-MS determination. Journal of Analytical Atomic Spectrometry, 2019, 34, 915-921.	1.6	23
17	Chemical Analysis and Imaging of Fingerprints by Air-flow Assisted Desorption Electrospray Ionization Mass Spectrometry. Chinese Journal of Analytical Chemistry, 2019, 47, 1909-1914.	0.9	5
18	Determination of Trace Mercury in Water by On-line Solid Phase Extraction and Ultraviolet Vapor Generation–ICP-MS. Atomic Spectroscopy, 2019, 40, 37-41.	0.4	6

#	Article	IF	CITATIONS
19	Acute Oral Administration of Singleâ€Walled Carbon Nanotubes Increases Intestinal Permeability and Inflammatory Responses: Association with the Changes in Gut Microbiota in Mice. Advanced Healthcare Materials, 2018, 7, e1701313.	3.9	40
20	Concentration of chromium in whole blood and erythrocytes showed different relationships with serum apolipoprotein levels in Cr(VI) exposed subjects. Journal of Trace Elements in Medicine and Biology, 2018, 50, 384-392.	1.5	10
21	Thermal Unfolding Process of Lysozyme on PEGylated Gold Nanoparticles Reveals Length-Dependent Effects of PEG Layer. Journal of Nanoscience and Nanotechnology, 2018, 18, 5542-5550.	0.9	1
22	Gut Microbiota: Acute Oral Administration of Singleâ€Walled Carbon Nanotubes Increases Intestinal Permeability and Inflammatory Responses: Association with the Changes in Gut Microbiota in Mice (Adv. Healthcare Mater. 13/2018). Advanced Healthcare Materials, 2018, 7, 1870053.	3.9	0
23	Transferrin Adsorbed on PEGylated Gold Nanoparticles and Its Relevance to Targeting Specificity. Journal of Nanoscience and Nanotechnology, 2018, 18, 5306-5313.	0.9	11
24	Inhibition of Lysozyme Fibrillation by Gold Nanorods and Nanoparticles. Journal of Nanoscience and Nanotechnology, 2018, 18, 3087-3094.	0.9	4
25	ZnO nanoparticles act as supportive therapy in DSS-induced ulcerative colitis in mice by maintaining gut homeostasis and activating Nrf2 signaling. Scientific Reports, 2017, 7, 43126.	1.6	76
26	Interrogating the variation of element masses and distribution patterns in single cells using ICP-MS with a high efficiency cell introduction system. Analytical and Bioanalytical Chemistry, 2017, 409, 1415-1423.	1.9	45
27	Manufactured nanoparticle: A prediction model for understanding PM2.5 toxicity to human. Green Energy and Environment, 2017, 2, 3-4.	4.7	2
28	The effects of orally administered Ag, TiO 2 and SiO 2 nanoparticles on gut microbiota composition and colitis induction in mice. NanoImpact, 2017, 8, 80-88.	2.4	139
29	Elemental Bio-imaging of Biological Samples by Laser Ablation-Inductively Coupled Plasma-Mass Spectrometry. Chinese Journal of Analytical Chemistry, 2016, 44, 1646-1651.	0.9	3
30	Size-Dependent Translocation Pattern, Chemical and Biological Transformation of Nano- and Submicron-Sized Ferric Oxide Particles in the Central Nervous System. Journal of Nanoscience and Nanotechnology, 2016, 16, 5553-5561.	0.9	22
31	Chirality of Graphene Oxide–Humic Acid Sandwich Complex Induced by a Twisted, Long-Range-Ordered Nanostructure. Journal of Physical Chemistry C, 2016, 120, 25789-25795.	1.5	17
32	Magnetic Fe3O4 nanoparticle catalyzed chemiluminescence for detection of nitric oxide in living cells. Analytical and Bioanalytical Chemistry, 2016, 408, 5479-5488.	1.9	16
33	Coculture with Lowâ€Dose SWCNT Attenuates Bacterial Invasion and Inflammation in Human Enterocyteâ€like Cacoâ€2 Cells. Small, 2015, 11, 4366-4378.	5.2	18
34	Facile Approach To Observe and Quantify the α _{Ilb} β ₃ Integrin on a Single-Cell. Analytical Chemistry, 2015, 87, 2546-2549.	3.2	53
35	Quantitative analysis of Gd@C82(OH)22 and cisplatin uptake in single cells by inductively coupled plasma mass spectrometry. Analytical and Bioanalytical Chemistry, 2015, 407, 2383-2391.	1.9	42
36	Probing the interaction at nano-bio interface using synchrotron radiation-based analytical techniques. Science China Chemistry, 2015, 58, 768-779.	4.2	28

#	Article	IF	CITATIONS
37	Structure and catalytic activities of ferrous centers confined on the interface between carbon nanotubes and humic acid. Nanoscale, 2015, 7, 2651-2658.	2.8	7
38	Time-resolved ICP-MS analysis of mineral element contents and distribution patterns in single cells. Analyst, The, 2015, 140, 523-531.	1.7	76
39	Oral magnetite nanoparticles disturb the development of <i>Drosophila melanogaster</i> from oogenesis to adult emergence. Nanotoxicology, 2015, 9, 302-312.	1.6	43
40	Quantitative Analysis of Gold Nanoparticles in Single Cells by Laser Ablation Inductively Coupled Plasma-Mass Spectrometry. Analytical Chemistry, 2014, 86, 10252-10256.	3.2	73
41	Development of anion-exchange high-performance liquid chromatography-inductively coupled plasma mass spectrometry methods for the speciation analysis of inorganic selenium and iodine in groundwater. Analytical Methods, 2014, 6, 8380-8387.	1.3	4
42	Graphene oxide as an anaerobic membrane scaffold for the enhancement of <i>B. adolescentis</i> proliferation and antagonistic effects against pathogens <i>E. coli</i> and <i>S. aureus</i> . Nanotechnology, 2014, 25, 165101.	1.3	50
43	Broadâ€ S pectrum Antibacterial Activity of Carbon Nanotubes to Human Gut Bacteria. Small, 2013, 9, 2735-2746.	5.2	236
44	Physicochemical Origin for Free Radical Generation of Iron Oxide Nanoparticles in Biomicroenvironment: Catalytic Activities Mediated by Surface Chemical States. Journal of Physical Chemistry C, 2013, 117, 383-392.	1.5	131
45	Determination of quantum dots in single cells by inductively coupled plasma mass spectrometry. Talanta, 2013, 116, 782-787.	2.9	56
46	Metabolism of Nanomaterials <i>in Vivo</i> : Blood Circulation and Organ Clearance. Accounts of Chemical Research, 2013, 46, 761-769.	7.6	424
47	Metallomics insights for in vivo studies of metal based nanomaterials. Metallomics, 2013, 5, 793.	1.0	37
48	Reducing Poisson noise and baseline drift in x-ray spectral images with bootstrap Poisson regression and robust nonparametric regression. Physics in Medicine and Biology, 2013, 58, 1739-1758.	1.6	11
49	Study of Reaction Dynamics Between Bovine Serum Albumin and Cisplatin by Size Exclusion Chromatography-Inductively Coupled Plasma-Mass Spectrometry. Chinese Journal of Analytical Chemistry, 2013, 40, 1289-1292.	0.9	0
50	The distribution profile and oxidation states of biometals in APP transgenic mouse brain: dyshomeostasis with age and as a function of the development of Alzheimer's disease. Metallomics, 2012, 4, 289.	1.0	48
51	Immunogold labeling and X-ray fluorescence microscopy reveal enrichment ratios of Cu and Zn, metabolism of APP and amyloid-β plaque formation in a mouse model of Alzheimer's disease. Metallomics, 2012, 4, 1113.	1.0	20
52	Temperature-Controlled Synthesis of CdSe Nanocrystals with Narrow Size Distribution. Journal of Nanoscience and Nanotechnology, 2012, 12, 6301-6307.	0.9	0
53	Effects of Chronic Chromate Exposure on Human Serum Prostate Specific Antigen: A Cross Sectional Study. Industrial Health, 2012, 50, 95-102.	0.4	5
54	Exosomes as Extrapulmonary Signaling Conveyors for Nanoparticleâ€Induced Systemic Immune Activation. Small, 2012, 8, 404-412.	5.2	93

#	Article	lF	CITATIONS
55	Quantification of proteins using lanthanide labeling and HPLC/ICP-MS detection. Journal of Analytical Atomic Spectrometry, 2011, 26, 1233.	1.6	19
56	Endothelial dysfunction and inflammation induced by iron oxide nanoparticle exposure: Risk factors for early atherosclerosis. Toxicology Letters, 2011, 203, 162-171.	0.4	193
57	Microglial activation, recruitment and phagocytosis as linked phenomena in ferric oxide nanoparticle exposure. Toxicology Letters, 2011, 205, 26-37.	0.4	106
58	Renal impairment caused by chronic occupational chromate exposure. International Archives of Occupational and Environmental Health, 2011, 84, 393-401.	1.1	37
59	Structural and functional insights into polymorphic enzymes of cytochrome P450 2C8. Amino Acids, 2011, 40, 1195-1204.	1.2	21
60	Vitamin B12 and folate deficiency and elevated plasma total homocysteine in workers with chronic exposure to chromate. Occupational and Environmental Medicine, 2011, 68, 870-875.	1.3	11
61	Chapter 4. Isotopic Techniques Combined with ICP-MS and ESI-MS. , 2010, , 95-127.		Ο
62	New methods for nanotoxicology: synchrotron radiation-based techniques. Analytical and Bioanalytical Chemistry, 2010, 398, 667-676.	1.9	32
63	ICPâ€MSâ€Based strategies for protein quantification. Mass Spectrometry Reviews, 2010, 29, 326-348.	2.8	103
64	Oxidative Stress and Apoptosis Induced by Iron Oxide Nanoparticles in Cultured Human Umbilical Endothelial Cells. Journal of Nanoscience and Nanotechnology, 2010, 10, 8584-8590.	0.9	109
65	<i>In Vitro</i> Cytotoxicity of Transparent Yellow Iron Oxide Nanoparticles on Human Glioma Cells. Journal of Nanoscience and Nanotechnology, 2010, 10, 8550-8555.	0.9	2
66	Using ion-pair reversed-phase HPLC ICP-MS to simultaneously determine Cr(III) and Cr(VI) in urine of chromate workers. Talanta, 2010, 81, 1856-1860.	2.9	72
67	Quantitative imaging of element spatial distribution in the brain section of a mouse model of Alzheimer's disease using synchrotron radiation X-ray fluorescence analysis. Journal of Analytical Atomic Spectrometry, 2010, 25, 328-333.	1.6	54
68	Particokinetics and Extrapulmonary Translocation of Intratracheally Instilled Ferric Oxide Nanoparticles in Rats and the Potential Health Risk Assessment. Toxicological Sciences, 2009, 107, 342-351.	1.4	188
69	Neurotoxicity of low-dose repeatedly intranasal instillation of nano- and submicron-sized ferric oxide particles in mice. Journal of Nanoparticle Research, 2009, 11, 41-53.	0.8	101
70	Acute toxicological impact of nano- and submicro-scaled zinc oxide powder on healthy adult mice. Journal of Nanoparticle Research, 2008, 10, 263-276.	0.8	338
71	Comparative study of pulmonary responses to nano- and submicron-sized ferric oxide in rats. Toxicology, 2008, 247, 102-111.	2.0	246
72	Analysis of mercury-containing protein fractions in brain cytosol of the maternal and infant rats after exposure to a low-dose of methylmercury by SEC coupled to isotope dilution ICP-MS. Journal of Analytical Atomic Spectrometry, 2008, 23, 1112.	1.6	23

#	Article	IF	CITATIONS
73	Development of a mild mercaptoethanol extraction method for determination of mercury species in biological samples by HPLC–ICP-MS. Talanta, 2007, 71, 2034-2039.	2.9	184
74	Quantitative Analysis of Proteins via Sulfur Determination by HPLC Coupled to Isotope Dilution ICPMS with a Hexapole Collision Cell. Analytical Chemistry, 2007, 79, 9128-9134.	3.2	77
75	The transport of chromium(III) in the body: Implications for function. , 2007, , 121-137.		5
76	Investigation of mercury-containing proteins by enriched stable isotopic tracer and size-exclusion chromatography hyphenated to inductively coupled plasma-isotope dilution mass spectrometry. Analytica Chimica Acta, 2007, 583, 84-91.	2.6	20
77	Determination of Mercury in Fish by Isotope Dilution Inductively Coupled Plasma-Mass Spectrometry. Chinese Journal of Analytical Chemistry, 2007, 35, 945-948.	0.9	10
78	Acute toxicity of nano- and micro-scale zinc powder in healthy adult mice. Toxicology Letters, 2006, 161, 115-123.	0.4	276
79	Isotopic Tracer Studies on the Metabolism and Functional Roles of Mineral Elements in Institute of High Energy Physics, China. Journal of Nuclear Science and Technology, 2006, 43, 450-454.	0.7	2
80	Mercury and trace element distribution in organic tissues and regional brain of fetal rat after in utero and weaning exposure to low dose of inorganic mercury. Toxicology Letters, 2004, 152, 223-234.	0.4	30
81	Study of chromium-containing proteins in subcellular fractions of rat liver by enriched stable isotopic tracer technique and gel filtration chromatography. Analytical and Bioanalytical Chemistry, 2003, 375, 363-368.	1.9	27
82	Tissue contents and subcellular distribution of chromium and other trace metals in experimental diabetic rats after intravenous injection of Cr 50[ndash]enriched stable isotopic tracer solution. Metabolism: Clinical and Experimental, 2001, 50, 1168-1174.	1.5	15
83	Comparison of the chromium distribution in organs and subcellular fractions of normal and diabetic rats by using enriched stable isotope Cr-50 tracer technique. Biological Trace Element Research, 1999, 71-72, 121-129.	1.9	12
84	Use of the enriched stable isotope Cr-50 as a tracer to study the metabolism of chromium (III) in normal and diabetic rats. Biological Trace Element Research, 1998, 63, 129-138.	1.9	23
85	Serum and urine chromium concentrations in elderly diabetics. Biological Trace Element Research, 1998, 63, 231-237.	1.9	43
86	Total and methyl mercury levels in human scalp hairs of typical populations in China by NAA, GC(EC), and other techniques. Biological Trace Element Research, 1994, 43-45, 423-433.	1.9	8